

Transmission loss of corrugated plates

Rafael Piscocoya, Martin Ochmann

Beuth Hochschule für Technik Berlin, University of Applied Sciences, Berlin, Germany.

Summary

The transmission loss of corrugated plates is computed by a coupled FEM-BEM approach. The normal vibrations of the plate are calculated with a FEM simulation. They are used as basis for the modal expansion of the displacement of the plate. The participation factors are determined solving the equation of motion of the plate including the fluid load. The load acting on the plate due to the sound pressure is determined using the BEM. The results of the model are compared to the results obtained by an approximated approach which treats the corrugated plate as a flat orthotropic plate with equivalent bending stiffness. The insulation of the corrugated plate is also compared with the insulation of a flat isotropic plate with the same thickness that covers the same area.

PACS no. 43.55.Ti, 43.20.Rz

1. Introduction

Corrugated plates have a wide range of applications in various branches of engineering due to their larger bending stiffness, e.g. in roof structures or in gas turbine enclosures. Such type of plates can be treated as orthotropic since the stiffness in the direction along the raised profile is much higher than in the perpendicular direction. Equivalent stiffness in each direction can be deduced from the geometry of the plate and the properties of the material. The sound radiation of the plate can be computed with a simple Rayleigh integral. Under those assumptions, formulas to predict the natural vibrations and the sound reduction from flat and profiled plates have been deduced in the past. In the present work, a numerical model for determining the transmission loss of corrugated plates which considers the geometry of the plate and calculates more accurately the sound radiation is developed. The natural vibrations of the plate in vacuum are previously determined with a FEM simulation and transferred to a BEM calculation of the sound radiation.

2. “Planification” approach

Corrugated plates can be modelled as orthotropic flat plates. Assuming that the bending wavelength is much larger than the “period” of the profile, the bending stiffness in the two orthogonal directions can be approximated in terms of the geometry and material properties of the plate.

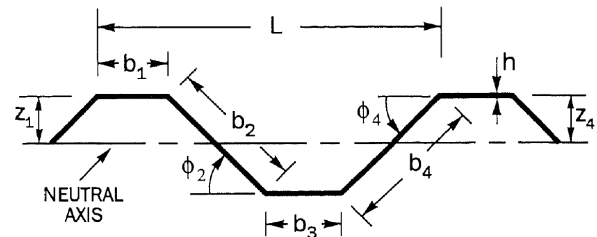


Figure 1. Corrugated plate profile, figure taken from [1]

With the parameters illustrated in Fig. 1, the bending stiffness across the profile can be written as [1]

$$B_x = \frac{Eh^3}{12(1-n^2)} \sum_n b_n \quad (1)$$

The stiffness along the profile can be calculated with the expression

$$B_y = \frac{Eh^3}{(1-n^2)L} \sum_n b_n^2 \left(z_n^2 + \frac{h^2 + b_n^2}{24} + \frac{h^2 - b_n^2}{24} \cos 2f_n \right) \quad (2)$$

and the stiffness B_{xy} is given by

$$B_{xy} = \frac{1}{2} \left(B_x n + B_y n + \frac{Gh^3}{3} \right) \quad (3)$$

The formula for the eigenfrequencies of a simply supported orthotropic plate reads

$$f_{mn} = \frac{p/2}{\sqrt{rh}} \left[\frac{m^4 B_x}{a^4} + \frac{n^4 B_y}{b^4} + \frac{2m^2 n^2}{a^2 b^2} B_{xy} \right]^{1/2} \quad (4)$$

where a and b are the dimensions of the plate. The eigenfrequencies of a simply supported corrugated plate can be obtained from (4) using the equivalent bending stiffness given in (1)-(3). However, the assumption of a much larger bending wavelength does not hold for high frequencies. Thus, it is expected that (4) only gives reasonable values for the lower eigenfrequencies.

3. Accurate acoustic model

The following model does not consider any approximation and takes into account the form of the plate for the calculation of the sound radiation. We study a thin plate with trapezoid profile (cladding) but the model can handle any arbitrary geometry. The plate is embedded in an infinite baffle. A plane wave with incident angle θ excites the plate and the vibration of the plate produces sound at both sides of the plate.

The displacement of the plate u satisfies the equation of motion

$$(K - \omega^2 M)u = F \quad , \quad (5)$$

where K and M are the stiffness and mass matrices, and F is the vector of the external forces.

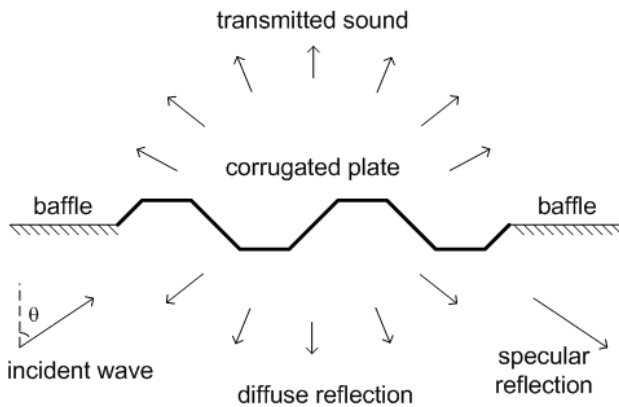
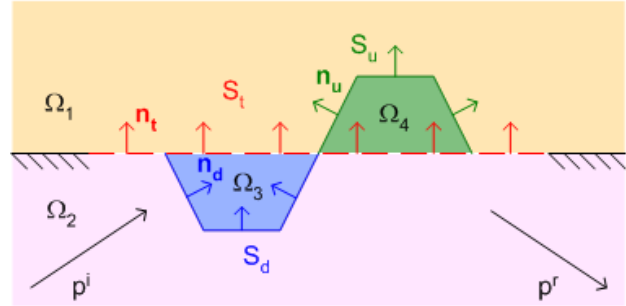


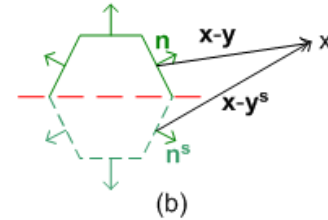
Figure 2. Corrugated plate in an infinite baffle.

In case of airborne sound transmission, F is proportional to the pressure difference above and below the plate. This difference can be calculated using integral equations. To formulate the proper equations, the space is divided in four subdomains as sketched in Fig. 3. It is important to distinguish the regions above and below the plane containing the baffle. The baffle provides a real surface to divide the space, but it is necessary to define a

fictitious surface S_t to account for the part of the plane occupied by the plate. Hence, above the plane the subdomains Ω_1 and Ω_4 are defined while the subdomains Ω_2 and Ω_3 are defined below the plane.



(a)



(b)

Figure 3. Description of the acoustic model; (a) subdomains, boundaries and normal vectors; (b) real and mirror image of source points and normal vectors.

In each subdomain, the sound pressure is given by an integral equation as follows [2]

$$C_1 p_1 = \int_{S_u} (p_1 \frac{\partial g^h}{\partial n_y} - r w^2 u g^h) dS_y - \int_{S_t} \frac{\partial p}{\partial n_y} g^h dS_y \quad , \quad \text{in } \Omega_1 \quad (6.a)$$

$$C_2 p_2 = - \int_{S_d} (p_2 \frac{\partial g^h}{\partial n_y} - r w^2 u g^h) dS_y + \int_{S_t} \frac{\partial p}{\partial n_y} g^h dS_y + p^i + p^r \quad , \quad \text{in } \Omega_2 \quad (6.b)$$

$$C_3 p_3 = \int_{S_d} (p_3 \frac{\partial g^h}{\partial n_y} - r w^2 u g^h) dS_y + \int_{S_t} \frac{\partial p}{\partial n_y} g^h dS_y \quad , \quad \text{in } \Omega_3 \quad (6.c)$$

$$C_4 p_4 = - \int_{S_u} (p_4 \frac{\partial g^h}{\partial n_y} - r w^2 u g^h) dS_y - \int_{S_t} \frac{\partial p}{\partial n_y} g^h dS_y \quad , \quad \text{in } \Omega_4 \quad (6.d)$$

where g^h and $\partial g^h/\partial n_y$ correspond to the Green's function for the halfspace and its normal derivative with respect to the vector y :

$$g^h(x, y) = \frac{e^{-jk|x-y|}}{4p|x-y|} + \frac{e^{-jk|x-y^s|}}{4p|x-y^s|} \quad , \quad (7)$$

$$\begin{aligned} \frac{\partial g^h}{\partial n_y}(x, y) &= (1 + jk|x-y|) \frac{e^{-jk|x-y|}}{4p|x-y|^2} \frac{(x-y) \cdot n_y}{|x-y|} \\ &+ (1 + jk|x-y^s|) \frac{e^{-jk|x-y^s|}}{4p|x-y^s|^2} \frac{(x-y^s) \cdot n_y^s}{|x-y^s|} \quad , \quad (8) \end{aligned}$$

and y^s and n^s denote the mirror image of the source point and the normal vector (see Fig. 3b).

Table I: Coefficients C_i

	C_1	C_2	C_3	C_4
S_u	0.5	0	0	0.5
S_d	0	0.5	0.5	0
S_t	1 ^a	1 ^b	1 ^c	1 ^d

^a S_t not in Ω_4 (otherwise 0) , ^b S_t not in Ω_3 (otherwise 0)

^c S_t in Ω_3 (otherwise 0) , ^d S_t in Ω_4 (otherwise 0)

To obtain the system of equations to be solved, equations (5) and (6.a)-(6.d) need to be discretized. There are six unknown variables $p_1, p_2, p_3, p_4, \partial p/\partial n$ on S_t and u on the plate, therefore, six equations are needed. The first equation can be obtained requiring continuity of the pressure on S_t .

$$(6.a)+(6.d) = (6.b)+(6.c) \quad \text{on } S_t \quad . \quad (9)$$

The second and third equations are obtained discretizing (6.b) and (6.c) on S_u and S_d respectively. Since the plate is very thin, the normal velocity at both sides of the plate is the same. Hence, the fourth and fifth equations are obtained by taking the derivative of Eqs. (6)

$$\frac{1}{2} \left(\frac{\partial p_1}{\partial n_x} + \frac{\partial p_4}{\partial n_x} \right) = r w^2 u \quad \text{on } S_u \quad , \quad (10.a)$$

$$\frac{1}{2} \left(\frac{\partial p_2}{\partial n_x} + \frac{\partial p_3}{\partial n_x} \right) = r w^2 u \quad \text{on } S_d \quad . \quad (10.b)$$

The force acting on the plate is due to the pressure difference above and below the plate

$$F = \int_S \Delta p \mathbf{n} dS_y \quad . \quad (11)$$

The pressure difference Δp is p_1-p_4 on S_u and p_3-p_2 on S_d . The sixth equation is obtained discretizing (5) and replacing (11) on the right hand side of (5). By combining all equations, a single equation for the displacement of the plate can be derived

$$(K + jwD - w^2M)u = b \quad . \quad (12)$$

where jwD is the load of the fluid on the plate and b is the excitation due to the incident plane wave.

To reduce the size of the matrix to be inverted, a modal expansion of the displacement u is introduced

$$u = \sum_n d_n f_n \quad , \quad (13)$$

where f_n is the n -th eigenmode of the plate in vacuum.

4. Numerical example

The developed numerical model was applied to a corrugated steel plate with thickness $h=3$ mm. The dimensions of the profile are shown in Fig. 4. The plate had eight repetitions of the profile, i.e. a total width of 2 m and each profile has a length of 3 m.

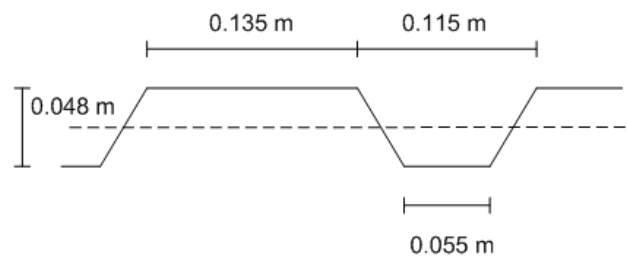


Figure 4. Dimensions of the profile.

For the numerical simulation, a mesh with 3510 nodes, 2968 elements and a maximum edge length of 0.057 m was generated.

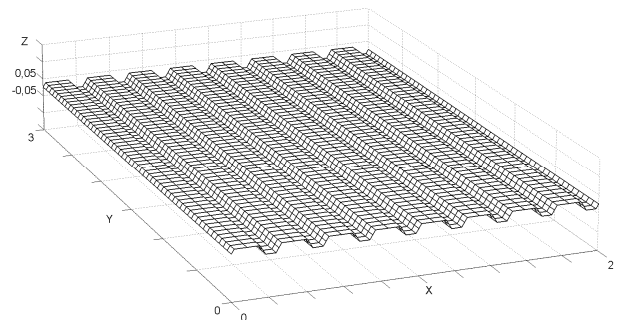


Figure 5. Mesh for the FEM and BEM calculations.

Two different boundary conditions were investigated: simply supported and clamped.

The eigenfrequencies and vibration modes of the profiled plate were obtained with a FEM simulation. In Table II, the first five simulated eigenfrequencies of the profiled plate are compared with the values obtained with formula (4). Only the first two values obtained with the approximated approach are near the numerical values. The displacement of the plate by these modes is illustrated in Fig. 6. From the third mode on, the deviations grow with increasing frequency. For the flat plate instead, the agreement between the FEM simulation and the analytical solution is very good (see Table III).

Table II: Eigenfrequencies of the profiled plate

Mode	(1,1)	(2,1)	(3,1)	(4,1)	(5,1)
numeric	40.4	43.3	49.1	58.6	72.1
formula	35.2	53.8	75.9	100.1	126.1

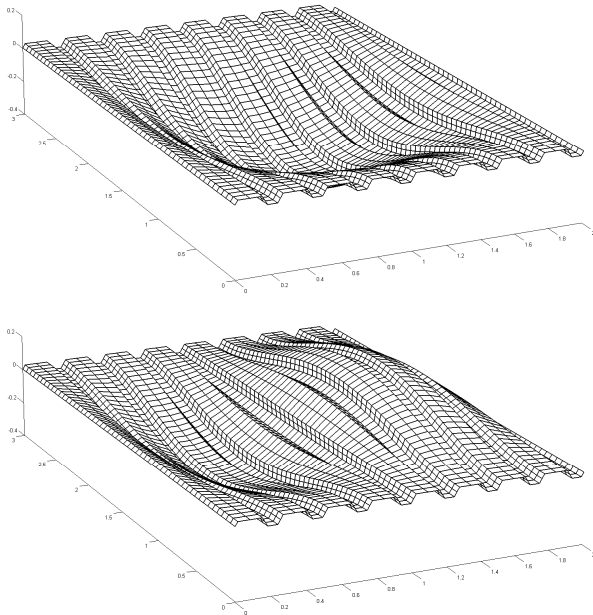


Figure 6. First (top) and second (bottom) eigenmode of the simply supported profiled plate.

Table III: Eigenfrequencies of the flat plate

Mode	(1,1)	(1,2)	(2,1)	(1,3)	(2,2)
formula	2.6	5.1	8.2	9.2	10.6
numeric	2.7	5.1	8.2	9.2	10.6

Following the planification approach, equivalent bending stiffness can be derived for the corrugated plate. Using (1) and (2) we obtain $B_x=425.8 \text{ N}\cdot\text{m}$, and $B_y=541380 \text{ N}\cdot\text{m}$. According to these values, two coincidence frequencies at $f_{cy}=123 \text{ Hz}$ and $f_{cx}=4400 \text{ Hz}$, which cover an important part of the audio range, are expected. In this region, the insulating behaviour of the plate is not optimum [3].

The transmission loss of the plate is defined as

$$R = -10 \log_{10} \left(\frac{W_{out}}{W_{inc}} \right) \quad (14)$$

where W_{out} is the radiated power and W_{inc} the incident power. The expressions of the power are given by

$$W_{out} = \frac{1}{2} \int_{S_u+S_d} \text{Re}(-j\omega p_{out} u^*) dS \quad , \quad p_{out} = [p_1^{S_u} \quad p_2^{S_d}]^T \quad ,$$

$$W_{inc} = \frac{1}{2rc} \int_{S_u+S_d} |p|^2 n_w \cdot n \quad dS \quad . \quad (15)$$

n_w is the unit vector in the direction of the plane wave and n the normal vector of the plate.

The transmission loss of the corrugated plate is presented in Figs. 7 and 8. In all cases, a single plane wave with incident angle $\theta=30^\circ$ is considered. The transmission loss due to a diffuse incident field can be calculated integrating over different incident angles. First, we compare R obtained with the approximated approach and with the numerical model (Fig. 7). We observe that the approximated approach provides a higher transmission loss in almost all 1/3 octave bands. The difference lies between 2 and 4 dB in average.

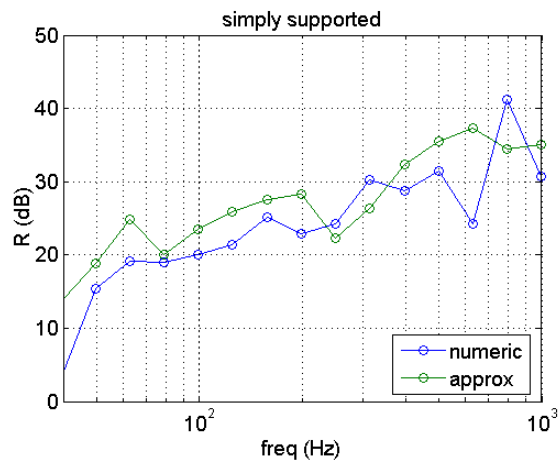


Figure 7. Comparison of the curves of transmission loss calculated with two models.

Next, we compare the transmission loss of the profiled plate with the transmission loss of the flat plate for the two cases: simply supported and clamped. In both cases, the flat plate has a better insulation as the profiled plate. The transmission loss of the flat plate increases approximately 6 dB/octave, while the transmission loss of the corrugated plate also increases but shows some oscillations.

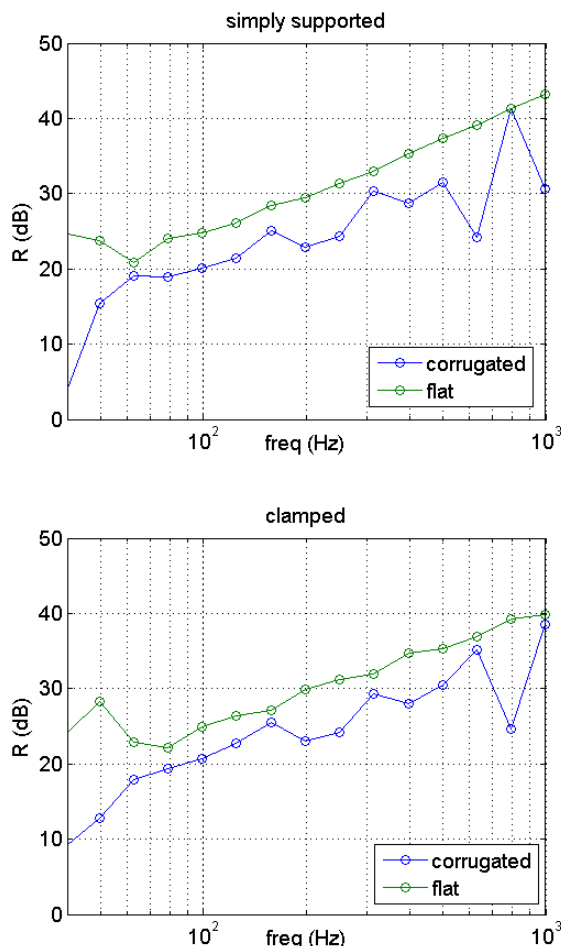


Figure 8. Transmission loss of corrugated and flat plates for simply supported (top) and clamped (bottom) boundary conditions.

5. Conclusions

The results presented in this article show that with the “planification” of the corrugated plate, only the first eigenfrequencies of the plate are calculated with reasonable accuracy and the values of the transmission loss tend to be overestimated. With the numerical model, a more accurate determination of the insulation of corrugated plates is possible.

The higher stiffness of corrugated plates has its downside on the lower transmission loss compared to flat plates. It is possible to improve the

insulation of corrugated plates inserting absorption material [3]. This feature will be implemented in a future work.

Acknowledgements

This work was supported by the German Research Foundation (DFG) within the project “The acoustical transmission problem for plate-like structures” (ATMOS).

Literature

- [1] C. Hansen: Sound Transmission Loss of corrugated panels. *Noise Control Engineering Journal*, Vol. 40 (1993), 187-197.
- [2] A. Seybert, T. W. Wu: Modified Helmholtz integral equation for bodies sitting on an infinite plane. *J. Acoust. Soc. Am* 85 (1989), 19-23.
- [3] C. Soares: *Process engineering equipment handbook*. Mc Graw-Hill, 2002.